Analyst

ROYAL SOCIETY OF CHEMISTRY

PAPER

View Article Online
View Journal | View Issue

Cite this: *Analyst*, 2021, **146**, 1924

In situ detection of plasma exosomal microRNA for lung cancer diagnosis using duplex-specific nuclease and MoS_2 nanosheets†

Zibo Gao,‡[a] Huijie Yuan,‡[a] Yanhua Mao,[a] Lihua Ding,[a] Clement Yaw Effah,[a] Sitian He,[a] Leiliang He,[a] Li-e Liu,[a] Songcheng Yu,[a] Yilin Wang,[a] Jia Wang,[a] Yongmei Tian,[a] Fei Yu,[a] Hongchao Guo,[a] Lijun Miao,[b] Lingbo Qu[c] and Yongjun Wu *[a]

Received 7th November 2020,
Accepted 21st December 2020

DOI: 10.1039/d0an02193h

rsc.li/analyst

MicroRNAs (miRNAs) encapsulated in tumor-derived exosomes are becoming ideal biomarkers for the early diagnosis and prognosis of lung cancer. However, the accuracy and sensitivity are often hampered by the extraction process of exosomal miRNA using traditional methods. Herein, this study developed a fluorogenic quantitative detection method for exosomal miRNA using the fluorescence quenching properties of molybdenum disulfide (MoS_2) nanosheets and the enzyme-assisted signal amplification properties of duplex-specific nuclease (DSN). First, a fluorescently-labeled nucleic acid probe was used to hybridize the target miRNA to form a DNA/RNA hybrid structure. Under the action of the DSN, the DNA single strand in the DNA/RNA hybrid strand was selectively digested into smaller oligonucleotide fragments. At the same time, the released miRNA target triggers the next reaction cycle, so as to achieve signal amplification. Then, MoS_2 was used to selectively quench the fluorescence of the undigested probe leaving the fluorescent signal of the fluorescently-labeled probe fragments. The fluorometric signals for miRNA-21 had a maximum excitation/emission wavelength of 488/518 nm. Most importantly, the biosensor was then applied for the accurate quantitative detection of miRNA-21 in exosome lysates extracted from human plasma and this method was able to successfully distinguish lung cancer patients from healthy people. This biosensor provides a simple, rapid, and a highly specific quantitative method for exosomal miRNA and has promising potential to be used in the early diagnosis of lung cancer.

Introduction

According to the World Health Organization's statistical report, lung cancer is the most common malignance with poor prognosis.[1] Most patients with lung cancer are usually diagnosed at the advanced stage, resulting in a reduced five-year survival rate of only 5%. However, according to Siegel *et al.*, this five-year survival rate of lung cancer patients at the localized stage can reach about 57%.[2] In order to achieve this, it is imperative to explore an effective early detection strategy for lung cancer. Exosomes are nanosized extracellular vesicles (30–150 nm) which carry abundant nucleic acids, proteins, and lipids and are considered as transmitters of information among cells.[3–5] Among these biomolecules, exosomal microRNAs (miRNAs) are one of the potential biomarkers, which play an important role in the transmission of information in tumor growth and metastasis.[6] Most importantly, miRNAs that are encapsulated in the exosomal lipid bilayer are protected from degradation by ribonuclease in the body fluids. Therefore, several studies have suggested that exosomal miRNA (*e.g.* miRNA-155, miRNA-210 and miRNA-21, *etc.*) could be used for the screening and prediction prognosis of a variety of human tumors, including lung cancer.[7–10]

However, due to the high homology among family members coupled with their relatively short length, and low abundance, it is challenging to accurately quantify miRNAs. There are three common methods used for the detection of miRNA. These include northern blotting, reverse transcription-polymerase chain reaction (RT-PCR), and microarrays. However, these methods have their detection limits. Northern

[a]*College of Public Health, Zhengzhou University, Zhengzhou 450001, China. E-mail: wuyongjun135@126.com; Tel: +86-371-67781450;; Fax: +86-371-67781450*
[b]*The First Affiliated Hospital of Zhengzhou University, Zhengzhou 450052, China*
[c]*Henan Joint International Research Laboratory of Green Construction of Functional Molecules and Their Bioanalytical Applications, Zhengzhou University, Zhengzhou, 450001, China*

†Electronic supplementary information (ESI) available. See DOI: 10.1039/d0an02193h

‡These authors contributed equally to this work.

blotting has numerous limitations which include, low-throughput, low sensitivity, and it is time-consuming.[11] RT-PCR is complicated, expensive, unstable, and prone to false positives.[12,13] Also, the high cost of microarrays and the poor specificity of miRNAs to detect similar sequences are notable.[14,15] At present, the quantitative methods involving exosomal miRNAs are mostly carried out by exosome cleavage, RNA extraction and reverse transcription of cDNA.[7,16] This method is easily limited by the amount of RNA extracted and the degradation of RNA during the extraction process.[17] Meanwhile, in the early stages of lung cancer, the expression level of exosome miRNA is low. Also, the currently accepted methods for the isolation of exosomes can be faced with some challenges which include but are not limited to time-consuming, protein contamination and low yield of exosomes. Therefore, an *in situ* detection method which is simple, rapid, and accurate and has a high signal-to-noise ratio may be a better choice for the quantitative detection of exosomal miRNA. There are a number of novel technologies that have been recently developed, which generally used an electrochemical or optical detection system.[18–21] Among these novel methods, fluorescence detection has the following advantages: the use of simple instrument, rapid operation and a high selectivity. Some studies have established fluorescence detection methods for exosome miRNA.[18,22] However, without combining the fluorescent probe with the signal amplification reagent, its high detection sensitivity and the limit of detection will suffer great limitation.[23,24]

Duplex-specific nuclease (DSN) is a stable nuclease which can selectively digest the DNA strands of double-stranded nucleic acids, rather than digest RNA in DNA–RNA heteroduplexes, while also being able to distinguish a single base difference between perfectly matched and incompletely matched DNA double strands. However, it does not work on single-stranded DNA and single-stranded RNA.[25,26] DSN can digest the DNA only when DNA pairing of more than 10 bp in double-stranded DNA or when DNA pairing of 15 bp in DNA–RNA heteroduplexes takes place.[27] According to Zhao, this digestion was sequence independent and the digested products may consist of a plenty of short nucleotide chains (<10 bp) and a few mononucleotides.[28] Based on these particular advantages, the DSN has shown great application potential in the detection of miRNA signal amplification.[29,30]

Molybdenum disulfide (MoS_2) is a graphene-like two-dimensional sheet material. Research shows that compared with graphene, MoS_2 nanosheets are more easily dispersed in water solution without additional complex treatments such as the use of surfactants or oxidation, and are more applicable for large-scale production.[31,32] Due to the advantages of good biocompatibility, easy functional modification and high quenching efficiency for fluorescent substances, MoS_2 can improve the sensitivity of biosensors and shows great potential for application in chemical biosensing.[33–35] For the first time, Zhu *et al.* have shown that MoS_2 nanosheets quench fluorescence of a fluorescently tagged single-stranded DNA but not of a double-stranded DNA.[31] Lu *et al.* adsorbed the carcinoma embryonic antigen (CEA) aptamer to the surface of the MoS_2 nanosheet based on the van der Waals force interactions, and the fluorescence signal of the aptamer was quenched by fluorescence resonance energy transfer, realizing a high specificity and high sensitivity detection of CEA in the range of 100 pg mL^{-1}–100 ng mL^{-1}.[36] Fan Yang *et al.* established miRNA-21 and pre-miRNA-21 fluorescence imaging methods in living cells by functionalizing MoS_2 nanosheets with aptamers AS1411 and polyethylene glycol, and co-loading two engineered molecular beacon gene probes.[37]

Despite the success achieved in various detection methods for exosomal miRNA, there is still more work that needs to be done. This study aims to establish a detection method for exosomal miRNA by developing a new, rapid and a sensitive method that combines the fluorescence quencher, MoS_2 nanosheets with the enzyme-assisted signal amplifier, DSN. The detection strategy was divided into two parts: signal amplification based on DSN and fluorescence reaction based on MoS_2 nanosheets. First, a DNA/RNA hybrid structure was formed by the hybridization of the fluorescently-labelled nucleic acid probe and the target miRNA. The single stranded DNA in the DNA/RNA hybrid strand was then digested into smaller oligonucleotide fragments by the action of DSN. At the same time, the released target miRNA triggers the next reaction cycle, forming a new cycle for signal amplification. Then, the fluorescence of the undigested fluorescently-labelled probe was quenched after the MoS_2 nanosheet was added leaving the fluorescent signal of the fluorescently-labelled probe fragments. This assay detects exosomal miRNA *in situ* without RNA extraction, and the experimental system is simple, one-pot, and does not need repeated cleaning and filtration. The establishment and performance assessment of this method was finalised when it was able to subsequently analyze miRNA-21. Some studies have established detection methods for MiRNA, but have not been able to apply it to actual clinical samples. Therefore, miRNA-21 was selected for the analysis of exosomes isolated from the plasma of nine lung cancer patients and three healthy controls. Finally, we also apply this method to simultaneously detect both miRNA-21 and miRNA-210.

Materials and methods

Reagents and materials

DSN was purchased from Evrogen (Russia). MoS_2 (product number: XF138) was obtained from Nanjing XFNANO Materials Tech Co., Ltd (Nanjing, China). The recombinant RNase inhibitor and RNase-free water were purchased from Takara Biotechnology Co., Ltd (Dalian, China). Tris (hydroxymethyl) aminomethane was obtained from Beijing Solarbio Science & Technology Co., Ltd (Beijing, China). DL-Dithiothreitol (DTT) was purchased from Aladdin (Shanghai, China). Ethylene diamine tetraacetic acid (EDTA) was obtained from BioFroxx (Germany). The water used in the experiments was deionized water. All other chemicals were of at least

Table 1 Oligonucleotide sequences

Name	Sequence (5′ to 3′)
FAM-Probe 21	FAM-CGT CAA CAT CAG TCT GAT AAG CTA TTG ACG
TAMRA-Probe 210	TAMRA-CGT CAG CCG CTG TCA CAC GCA CAG CTG ACG
miRNA-21	UAG CUU AUC AGA CUG AUG UUG A
microRN-210	CUG UGC GUG UGA CAG CGG CUG A
miRNA-21mismatch 1	UAG CUU AUC ACA CUG AUG UUG A
miRNA-21mismatch 2	UAG CUU AUA AGA CUA AUG UUG A
miRNA-21mismatch 3	UAG AUU AUC AUA CUG AUA UUG A
miRNA-21mismatch 4	UAA ACC AUCCCA CUCGGC GGC A
miRNA-21-3p	CAA CAC CAG UCG AUG GGC UGU

Underlined parts were the mismatched bases.

analytical grade. DSN and DTT were dissolved with deionized water to obtain 1× DSN master buffer (pH 8.0, 50 mM Tris, 5 mM $MgCl_2$, 1 mM DTT). EDTA was dissolved with deionized water to obtain 2× DSN stop buffer (10 mM EDTA). The detection of miRNA-21 was done in Tris-HCl buffer (10 mM $MgCl_2$, 20 mM Tris, 300 mM NaCl, pH 8.0). The FAM-probe 21, TAMRA-probe 210, miRNA-21, miRNA-210, miRNA-21mismatch 1 (M1), miRNA-21mismatch 2 (M2), miRNA-21mismatch 3 (M3), miRNA-21mismatch 4 (M4), and miRNA-21-3p (M3p) were prepared and purchased from Sangon Biotech Co., Ltd (Shanghai, China).

Two fluorescence labelling probes were designed as hairpin-shaped. The sequences for the nucleic acids are listed in Table 1. All experiments of human blood plasma were performed in accordance with the Guidelines of Helsinki Declaration and approved by the Ethics Committee of Zhengzhou University of China. Informed consents were obtained from human participants of this study.

Apparatus

A fluorescence spectrophotometer (FS5, Edinburgh Instruments, England) with an excitation wavelength of 488 nm and an emission scanning range of 500–600 nm for FAM was employed for the fluorescence measurements. For the TAMRA florescence probe, the spectral detection was carried out at an emission wavelength of 550 nm and an emission scanning range of 560–650 nm. Ultracentrifuge (Optima XPN-100, Beckman Coulter, USA) was used to purify exosomes. Transmission electron microscopy (TEM) (JEM-2100, Jeol, Tokyo, Japan) and the Nanoparticle Tracking Analysis System (NTA) (Nanosight NS300, Malvern Company, England) were used for the characterization of isolated exosomes.

Exosomes extraction from human plasma

A total of twelve clinical plasma samples (three healthy donors and nine patients with lung cancer) were obtained from the Department of Respiratory Medicine, The First affiliated Hospital of Zhengzhou University, Henan, China. The lung cancer types of nine lung cancer donors are all lung adenocarcinoma that include two stage IIIa patients and seven stage IV patients. 1 mL of plasma specimens were drawn from whole blood samples after centrifugation at 4000 rpm for 10 min. The exosomes of the plasma were extracted by differential ultracentrifugation. First, the plasma was diluted to 5 ml with PBS, followed by centrifugation at 300*g* for 10 min. The supernatant was then collected and centrifuged for 10 min at a centrifugal force of 2000*g*, followed by a 30 min centrifugation at 10 000*g*. Then, sediments were resuspended in PBS, following centrifugation at 110 000*g* for 90 min. A 0.22 μm pore filter was used to filter the resuspension followed by a centrifugal separation at 110 000*g* for 90 min. Finally, the sediments were resuspended and stored at −80 °C while the supernatant was discarded. All the centrifugations were performed at 4 °C. The collection of the plasma samples was approved by the ethics committee of the First affiliated Hospital of Zhengzhou University. All patients gave informed and written consent.

Characterization of exosomes

The morphology of exosomes was characterized by TEM. The protein concentration of isolated exosomes was quantified by the bicinchoninic acid (BCA) protein assay. Western blotting (WB) was used to detect the protein expressions of CD63 and Hsp70, which were, respectively, expressed on the membrane and in the lumen of the exosomes. NTA was used for the determination of concentration and the size of isolated exosomes. All samples were tested in 3 replicates.

Detection of miRNAs

Monoplex detection of miRNA-21 was initially performed. First, FAM-probe 21 (5 μL 1 μmol L^{-1}), DSN (0.2 U) and miRNA-21 were added to 1× DSN master buffer in a water bath at 45 °C for 1 h, and then slowly cooled to room temperature. Then, 2× DSN stop buffer (10 μL) was added and incubated for 20 min in order to stop the enzymatic reaction. Afterwards, Tris-HCl buffer and MoS_2 were added to the product of the enzymatic reaction and then incubated for 90 min at room temperature. Finally, the fluorescence of the products was measured. RNase-free tubes were used as the reaction vessel in these analyses. To demonstrate the multiplex detection potential of this method on miRNAs, two capture probes, FAM-probe 21 and TAMRA-probe 210 which, respectively, capture miRNA-21 and miRNA-210 were used. The two probes were added to the reaction system and the fluorescence intensities of FAM and TAMRA were measured.

Detection of miRNAs in exosomes

To obtain the exosome lysate, exosomes and Triton X-100 (0.3%) were mixed at a ratio of 1 : 1 and incubated at 4 °C for 30 min. Then, the exosome lysate was used for the *in situ* detection of miRNAs in exosomes (refer to step 2.5).

Results and discussion

The mechanism of miRNA fluorometric quantification

The principle of the *in situ* detection assay of miRNA is shown in Scheme. 1. The detection strategy is divided into two parts,

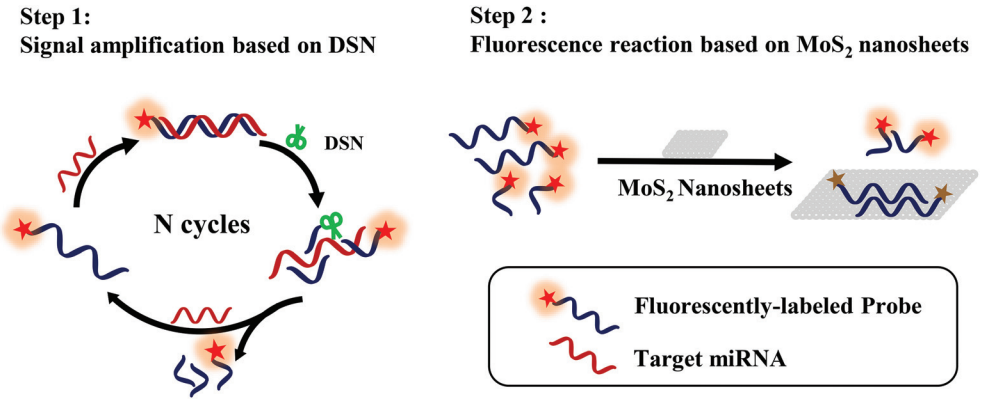

Scheme 1 Scheme of the fluorescence amplification for miRNAs based on MoS_2 and DSN.

signal amplification based on DSN and fluorescence reaction based on MoS_2 nanosheets. For the first part of this process, the fluorophore-labelled DNA probe hybridizes the targeted miRNA, followed by the DSN-mediated cleavage of the DNA probe of the DNA–RNA hybridized complex. Then, the target miRNA is released from the previously hybridized duplex, and new DNA–RNA heteroduplexes are generated because the force between the complementary DNA probe and the remaining RNA of DNA–RNA heteroduplexes is stronger than that of the digested nucleotide chain and single-stranded RNA. After a number of recycles of DSN-mediated hybridization, enzyme digestion and release, thousands of short ssDNA of various lengths (<10 bp) could be generated. EDTA was then used to inactivate the DSN. For the second step of this reaction, MoS_2 nanosheets were added. The fluorescence of intact probes was quenched when MoS_2 nanosheets were added to the reaction mixture. This quenching was made possible due to the adsorption property which is based on the van der Waals force interactions between the probes and the MoS_2 nanosheets. Yet, fluorophore-labelled fragments show strong fluorescence signalling because of the weak affinity between the cleaved short oligonucleotides and MoS_2 nanosheets.[38,39] Thus, the concentration of the target miRNA is proportionate to the fluorescence intensity cascade which is amplified by the cleavage behaviour of the DSN.

The feasibility of miRNA fluorometric quantification

We assessed the feasibility of miRNA fluorometric quantification (Fig. 1). The conditions with 25 nmol L^{-1} of FAM-probe 21, 35 μg mL^{-1} of MoS_2, 0.2 U of DSN, 45 °C of DSN reaction temperature, 60 min of DSN reaction time, and 30 min of MoS_2 incubation time were used in feasibility analysis. Curve a shows that fluorescence signalling was almost completely quenched after FAM-probe 21 was absorbed on MoS_2 nanosheets. Curve b shows that the DSN cannot retain the fluorescence signals of the probes in the reaction mixture without the presence of the target miRNA. Curve c indicates that the fluorophore-labelled probes retained a portion of the fluorescence signals in the reaction mixture containing

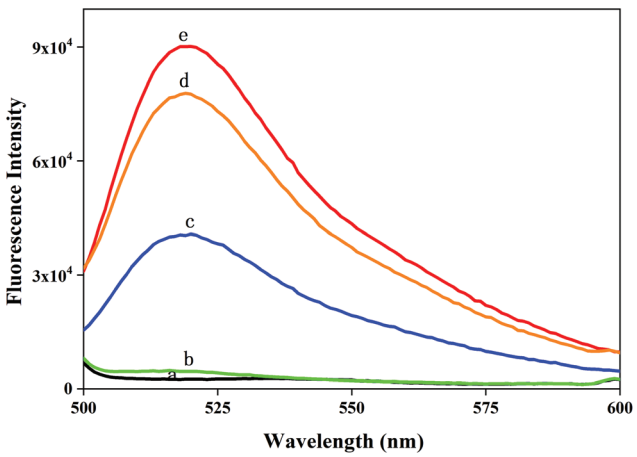

Fig. 1 Fluorescence spectrogram of FAM-probe 21 under different conditions. Curve a, FAM-probe 21 + MoS_2 nanosheets; curve b, FAM-probe 21 + MoS_2 nanosheets + DSN; curve c, FAM-probe 21 + MoS_2 nanosheets + miRNA-21; curve d, FAM-probe 21 + MoS_2 nanosheets + DSN + miRNA-21; curve e, FAM-probe 21 (25 nM).

miRNA-21, FAM-probe 21 and MoS_2 nanosheets. Finally, curve d indicates that fluorescence intensity could be amplified by DSN in the complete reaction system. These results powerfully demonstrate the feasibility of miRNA fluorometric quantification and signal amplification.

Characterization of exosomes

Exosomes were isolated from human plasma. The typical cup-shaped morphologies of the isolated exosomes were examined using TEM and the results are shown in Fig. S1A.† According to the results from Nanosight, the concentration of the isolated exosomes was about 1.88×10^{11} particles per mL (Fig. S1B†), and the mean diameter was 113.8 nm, which is similar to the exosome size in other reports.[9] Also, two exosomes protein markers, CD63 and HSP70, were identified by WB. The distinct bands validated the efficiency of the isolated exosome (Fig. S1C†). These results show that exosomes isolated from human plasma were typical.

The optimization of assay conditions

Optimization of the detection system for miRNA was performed by optimizing the concentrations of MoS_2 nanosheets and DSN, the reaction temperature of DSN, the reaction time of DSN, the fluorescence quenching and incubation time of MoS_2. Under the optimal concentration of MoS_2 nanosheets (Fig. 2A), the rate of fluorescence quenching was above 98%

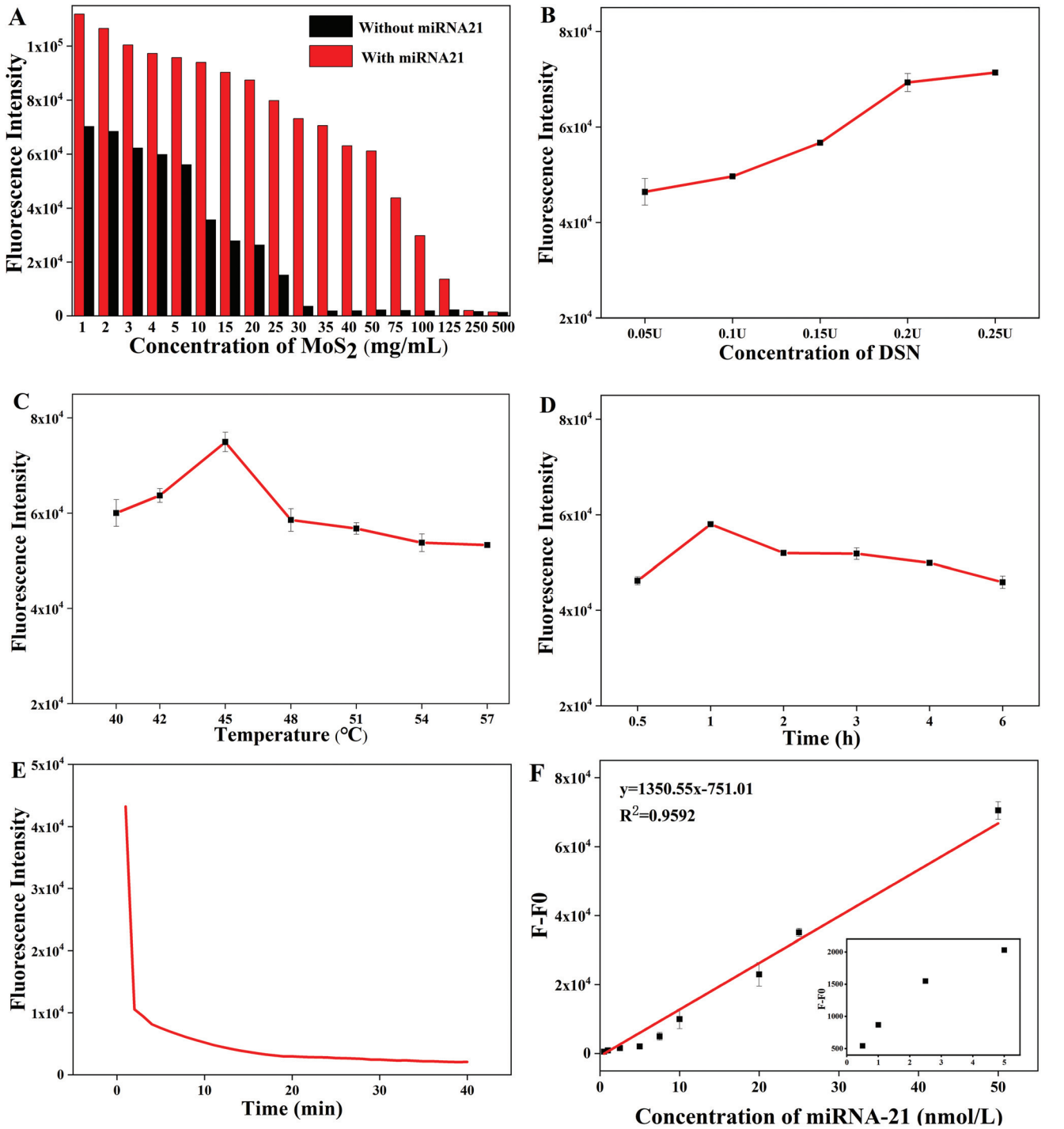

Fig. 2 (A) The optimization of the concentrations of MoS_2. Red bar: FAM-probe 21 (25 nM) + miRNA-21 (50 nM) + MoS_2. The black bar shows the absence of miRNA-21 when compared with the red bar. (B) The optimization of the concentrations of DSN. (C) The optimization of DSN incubation temperature. (D) The optimization of DSN incubation time. (E) The optimization of MoS_2 incubation time. (F) The standard curve between the concentration of miR-21 (0.5 nM, 1 nM, 2.5 nM, 5 nM, 7.5 nM, 10 nM, 20 nM, 25 nM, and 50 nM) and the fluorescence intensity. Inset: The amplified zone of the low concentration range of the calibration curve. The error bar shows the standard deviation of the three parallel tests.

and the rate of fluorescence recovery was above 58% when 35 μg mL^{-1} of MoS_2 was used. In order to ensure that the fluorescence of the fluorescence-labelled probes is completely quenched and that the fluorescent signals of the DSN-digested fragments remain strong, 35 μg mL^{-1} was selected as the optimized concentration for MoS_2 nanosheets. As the concentration of DSN increased from 0.05 U to 0.25 U, the fluorescence intensity also increased (Fig. 2B). When the concentration was higher than 0.2 U, the fluorescence intensity increased slowly. Thus, 0.2 U was selected as the optimal concentration for DSN. Next, the DSN reaction temperature (Fig. 2C) and reaction time (Fig. 2D) were optimized at 45 °C and 60 min, respectively, to achieve maximum fluorescence intensity. The fluorescence intensity was significantly reduced with an increasing reaction time, when MoS_2 was added to FAM-probe 21 (Fig. 2E). When the reaction time was longer than 20 min, the fluorescence intensity decreased slowly. In order to ensure that the fluorescence was completely quenched, 30 min was selected as the optimized fluorescence quenching time. Therefore, the optimum conditions chosen were 35 μg mL^{-1} of MoS_2, 0.2 U of DSN, 45 °C of DSN reaction temperature, 60 min of DSN reaction time, and 30 min of MoS_2 incubation time.

The sensitivity of miRNA fluorometric quantification

In order to determine the linearity between target miRNA and fluorescence intensity, the standard curve (Fig. 2F) of the different concentrations of miRNA-21 was established under the optimum conditions. The increment of the fluorescence intensity was linearly dependent on the concentrations of the target miRNA with the dynamic range of miRNA concentration varying from 0.5 nM to 50 nM, with a correlation equation of $y = 1350.55x + 1556.89$ ($R^2 = 0.9592$). The limit of detection (LOD) was 426 pM for miRNA-21 in the reaction system (LOD = $3\sigma/S$, 3σ = 3 times of the standard deviation of blank signal, S = slope of the standard curve).

The specificity of miRNA fluorometric quantification

Four similar mismatched targets of miRNA-21 and a homologous miRNA, M3p, were tested to investigate the selectivity of the platform under the optimum conditions. Four similar mismatched targets, including M1, M2, M3, and M4, had one, two, three and 13 mismatched bases, respectively. Fig. 3 shows that the fluorescence intensity of M1, M2, M3, M4, and M3p was five-fold lower than miRNA-21. Therefore, these results suggest that this platform has high specificity, and it could be used to quantify target miRNA in complex samples.

Detection of miRNAs in exosomes

Reports have suggested that miRNA-21 has a huge potential as a liquid biopsy biomarker in the identification and screening of lung cancer patients.[40] Based on this, miRNA-21 was selected for the analysis of exosomes isolated from the plasma of nine lung cancer patients and three healthy controls (shown in Table S1†). MiRNA-21 was successfully detected in exosome lysates (Fig. 4). The concentrations of miRNA-21 in the exosomes of the healthy controls group were lower than those of the lung cancer patients (as shown in Table S2†). These results suggest that this platform can selectively distinguish lung cancer patients from healthy people when detecting exosomal miRNA-21 extracted from plasma.

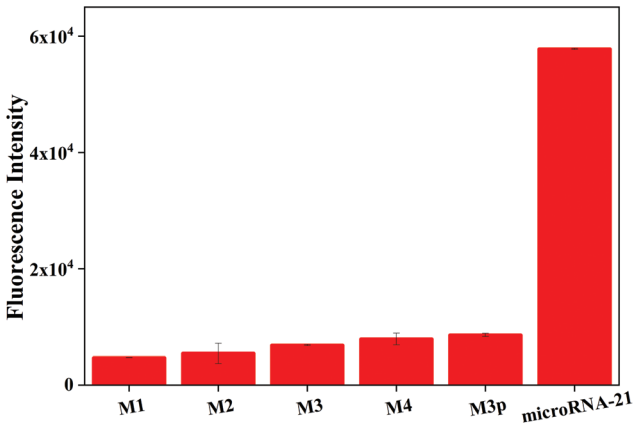

Fig. 3 The fluorescence intensity with five miRNAs (miR-21, M1, M2, M3, M4, and M3p) at 518 nm. The error bar shows the standard deviation of the three parallel tests.

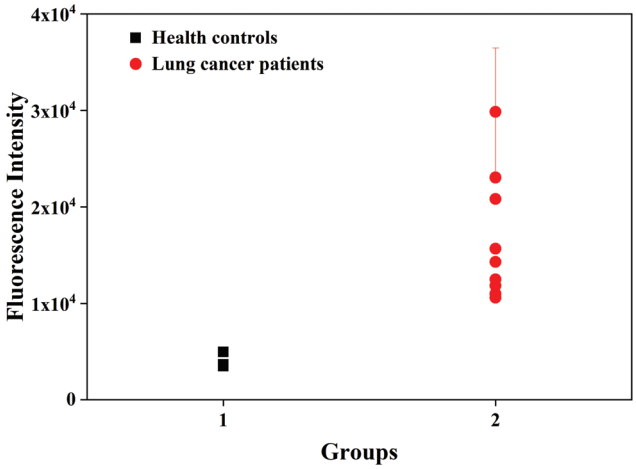

Fig. 4 The detection of miRNA-21 in exosomes. Group 1 exosomes isolated from healthy people. Group 2 exosomes isolated from lung cancer patients.

Multiplex detection of miRNA-21 and miRNA-210

MiRNA-21 and miRNA-210 are important regulators of cancer cells in the tumorigenesis and progress of lung cancer, such as proliferation and invasion of cancer cells and angiogenesis.[40,41]Therefore, a multiplexed assay that simultaneously quantifies both miRNA-21 and miRNA-210 was established (Fig. 5). We selected 518 nm and 580 nm to detect the fluorescence intensity of FAM-probe-21 and TAMRA-probe-210 separately. In the presence of two miRNAs, two bright fluorescent signals were simultaneously recorded at 518 nm and 580 nm (group 1) compared with the group which contains

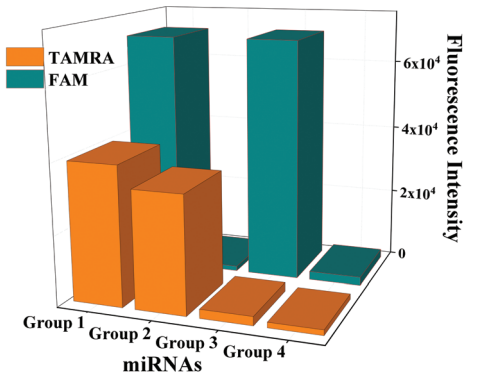

Fig. 5 The multiplexed assay simultaneously quantitating for miRNA-21 and miRNA-210. Group 1, miRNA-21 + miRNA-210. Group 2, miRNA-210. Group 3, miRNA-21. Group 4, without miRNA.

neither miRNA-21 nor miRNA-210 (group 4). In addition, when miRNA-21 or miRNA-210 exists alone, the fluorescence of FAM or TAMRA could be observed separately (group 2–3), showing the excellent recognition for miR-21 and miRNA210 in this strategy. Therefore, the result indicates that the fluorometric quantification assay is suitable for the multiplex detection of target miRNAs without any antagonistic influence of other miRNAs.

Conclusion

In this work, a simple, low-cost, and highly specific fluorescence detection method has been developed to detect exosomal miRNA *in situ*. The proposed detection platform performed well in real complex exosome lysates extracted from human plasma, and it successfully distinguished lung cancer patients from healthy people. Compared with the traditional detection methods of exosomal miRNA, this strategy does not depend on the complex RNA extraction process and polymerase chain reaction. It could quantitatively detect exosomal miRNA *in situ* without repeated cleaning and filtration, and only takes 150 minutes. Also, compared with the other miRNA detection methods which are based on a two-dimensional material, this assay used both the fluorescence signal amplification potential of DSN and the efficient background fluorescence quenching material, MoS_2, without using any quenching tag, making this method rapid, with a high specificity for the detection of exosomal miRNA. Furthermore, it was shown that this approach has the potential to be used in the multiplex detection of miRNAs in exosomes, and can provide easy quantification of exosomal miRNA with huge promising potential in the early diagnosis of lung cancer.

Abbreviations

miRNAs	MicroRNAs
MoS_2	Molybdenum disulfide
DSN	Duplex-specific nuclease
CEA	Carcinoma antigen
RT-PCR	Reverse transcription-polymerase chain reaction
DTT	DL-Dithiothreitol
M1	MiRNA-21mismatch 1
M2	MiRNA-21mismatch 2
M3	MiRNA-21mismatch 3
M4	MiRNA-21mismatch 4
M3p	MiRNA-21-3p
NTA	Nanoparticle tracking analysis system
TEM	Transmission electron microscopy
BCA	Bicinchoninic acid protein assay
WB	Western blotting
LOD	The limit of detection

Author contributions

Formal analysis and investigation: Zibo Gao and Huijie Yuan; writing – original draft preparation: Yanhua Mao and Zibo Gao; methodology: Sitian He and Lihua Ding; writing – review and editing: Clement Yaw Effaha, Leiliang He and Li-e Liu; resources: Songcheng Yu, Yilin Wang, Jia Wang, Yongmei Tian and Lingbo Qu; supervision: Hongchao Guo, Lijun Miao and Fei Yu; conceptualization: Yongjun Wu.

Conflicts of interest

There are no conflicts to declare.

Acknowledgements

This research was supported by the National Natural Science Foundation of China (No. 81573203) and the National Natural Science Foundation of China (No. 81973099).

References

1 F. Bray, J. Ferlay, I. Soerjomataram, R. L. Siegel, L. A. Torre and A. Jemal, *CA Cancer J. Clin.*, 2018, **68**, 394–424.
2 R. L. Siegel, K. D. Miller and A. Jemal, *CA Cancer J. Clin.*, 2020, **70**, 7–30.
3 H. Bu, D. He, X. He and K. Wang, *ChemBioChem*, 2019, **20**, 451–461.
4 D. K. Jeppesen, A. M. Fenix, J. L. Franklin, J. N. Higginbotham, Q. Zhang, L. J. Zimmerman, D. C. Liebler, J. Ping, Q. Liu, R. Evans, W. H. Fissell, J. G. Patton, L. H. Rome, D. T. Burnette and R. J. Coffey, *Cell*, 2019, **177**, 428–445.e18.
5 J. Kowal, M. Tkach and C. Théry, *Curr. Opin. Cell Biol.*, 2014, **29**, 116–125.
6 A. Sharma, Z. Khatun and A. Shiras, *Nanomedicine*, 2016, **11**, 421–437.
7 T. Matsumura, K. Sugimachi, H. Iinuma, Y. Takahashi, J. Kurashige, G. Sawada, M. Ueda, R. Uchi, H. Ueo,

Y. Takano, Y. Shinden, H. Eguchi, H. Yamamoto, Y. Doki, M. Mori, T. Ochiya and K. Mimori, *Br. J. Cancer*, 2015, **113**, 275–281.
8 Z. Lichner, A. Fendler, C. Saleh, A. N. Nasser, D. Boles, S. Al-Haddad, P. Kupchak, M. Dharsee, P. S. Nuin, K. R. Evans, K. Jung, C. Stephan, N. E. Fleshner and G. M. Yousef, *Clin. Chem.*, 2013, **59**, 1595–1603.
9 I. Vanni, A. Alama, F. Grossi, M. G. Dal Bello and S. Coco, *Drug Discovery Today*, 2017, **22**, 927–936.
10 L. Wu, W.-B. Zhou, J. Zhou, Y. Wei, H.-M. Wang, X.-D. Liu, X.-C. Chen, W. Wang, L. Ye, L. C. Yao, Q.-H. Chen and Z.-G. Tang, *Oncol. Lett.*, 2020, **20**, 1432–1440.
11 A. G. Torres, M. M. Fabani, E. Vigorito and M. J. Gait, *RNA*, 2011, **17**, 933–943.
12 H. Dong, J. Lei, L. Ding, Y. Wen, H. Ju and X. Zhang, *Chem. Rev.*, 2013, **113**, 6207–6233.
13 H.-L. Chen, M.-M. Guo, H. Tang, Z. Wu, L.-J. Tang, R.-Q. Yu and J.-H. Jiang, *Anal. Methods*, 2015, **7**, 2258–2263.
14 Y. Cheng, L. Dong, J. Zhang, Y. Zhao and Z. Li, *Analyst*, 2018, **143**, 1758–1774.
15 J. Ye, M. Xu, X. Tian, S. Cai and S. Zeng, *J. Pharm. Anal.*, 2019, **9**, 217–226.
16 H. Hu, H. Xu, F. Lu, J. Zhang, L. Xu, S. Xu, H. Jiang, Q. Zeng, E. Chen and Z. He, *Front. Bioeng. Biotechnol.*, 2020, **8**, 15.
17 L. Cheng, R. A. Sharples, B. J. Scicluna and A. F. Hill, *J. Extracell. Vesicles*, 2014, **3**, 23743.
18 H. Z. Wang, D. G. He, K. J. Wan, X. W. Sheng, H. Cheng, J. Huang, X. Zhou, X. X. He and K. M. Wang, *Analyst*, 2020, **145**, 3289–3296.
19 J. Zhao, C. Liu, Y. Li, Y. Ma, J. Deng, L. Li and J. Sun, *J. Am. Chem. Soc.*, 2020, **142**, 4996–5001.
20 S. Cho, H. C. Yang and W. J. Rhee, *Biosens. Bioelectron.*, 2019, **146**, 111749.
21 Q. Guo, Y. Yu, H. Zhang, C. Cai and Q. Shen, *Anal. Chem.*, 2020, **92**, 5302–5310.
22 J. Lee, M. H. Kwon, J. A. Kim and W. J. Rhee, *Artif. Cells, Nanomed., Biotechnol.*, 2018, **46**, S52–S63.
23 X. Cai, H. Zhang, X. Yu and W. Wang, *Talanta*, 2020, **216**, 120996.
24 D. Ma, C. Huang, J. Zheng, J. Tang, J. Li, J. Yang and R. Yang, *Biosens. Bioelectron.*, 2018, **101**, 167–173.
25 D. A. Shagin, D. V. Rebrikov, V. B. Kozhemyako, I. M. Altshuler, A. S. Shcheglov, P. A. Zhulidov, E. A. Bogdanova, D. B. Staroverov, V. A. Rasskazov and S. Lukyanov, *Genome Res.*, 2002, **12**, 1935–1942.
26 V. E. Anisimova, D. V. Rebrikov, D. A. Shagin, V. B. Kozhemyako, N. I. Menzorova, D. B. Staroverov, R. Ziganshin, L. L. Vagner, V. A. Rasskazov, S. A. Lukyanov and A. S. Shcheglov, *BMC Biochem.*, 2008, **9**, 14.
27 X. Qiu, H. Zhang, H. Yu, T. Jiang and Y. Luo, *Trends Biotechnol.*, 2015, **33**, 180–188.
28 Y. Zhao, H. Hoshiyama, J. W. Shay and W. E. Wright, *Nucleic Acids Res.*, 2008, **36**, e14.
29 B.-C. Yin, Y.-Q. Liu and B.-C. Ye, *J. Am. Chem. Soc.*, 2012, **134**, 5064–5067.
30 Y. Wang, P. D. Howes, E. Kim, C. D. Spicer, M. R. Thomas, Y. Lin, S. W. Crowder, I. J. Pence and M. M. Stevens, *ACS Appl. Mater. Interfaces*, 2018, **10**, 28290–28300.
31 C. Zhu, Z. Zeng, H. Li, F. Li, C. Fan and H. Zhang, *J. Am. Chem. Soc.*, 2013, **135**, 5998–6001.
32 J. Ge, E. C. Ou, R. Q. Yu and X. Chu, *J. Mater. Chem. B*, 2014, **2**, 625–628.
33 R. N. Dalila, M. K. Md Arshad, S. C. B. Gopinath, W. M. W. Norhaimi and M. F. M. Fathil, *Biosens. Bioelectron.*, 2019, **132**, 248–264.
34 A. Ganguly, J. Benson and P. Papakonstantinou, *ACS Appl. Bio Mater.*, 2018, **1**, 1184–1194.
35 G. Oudeng, M. Au, J. Shi, C. Wen and M. Yang, *ACS Appl. Mater. Interfaces*, 2018, **10**, 350–360.
36 L. J. Zhao, M. Cheng, G. N. Liu, H. Y. Lu, Y. Gao, X. Yan, F. M. Liu, P. Sun and G. Y. Lu, *Sens. Actuators, B*, 2018, **273**, 185–190.
37 F. Yang, P. Liu, X. Meng, H. Lu, Y. Cao, W. Dai, C. Wang and H. Dong, *Anal. Bioanal. Chem.*, 2019, **411**, 4559–4567.
38 M. Xiao, T. Man, C. Zhu, H. Pei, J. Shi, L. Li, X. Qu, X. Shen and J. Li, *ACS Appl. Mater. Interfaces*, 2018, **10**, 7852–7858.
39 M. Xiao, A. R. Chandrasekaran, W. Ji, F. Li, T. Man, C. Zhu, X. Shen, H. Pei, Q. Li and L. Li, *ACS Appl. Mater. Interfaces*, 2018, **10**, 35794–35800.
40 G. Rabinowits, C. Gerçel-Taylor, J. M. Day, D. D. Taylor and G. H. Kloecker, *Clin. Lung Cancer*, 2009, **10**, 42–46.
41 W. Zhu, K. Zhou, Y. Zha, D. Chen, J. He, H. Ma, X. Liu, H. Le and Y. Zhang, *PLoS One*, 2016, **11**, e0153046.